TSG-RAN WG4 meeting AH#4 **R4-103856**
Xi'an, China, 11th – 15th October 2010

Source:	Elektrobit
Title:	Verified Performance: Anechoic chamber and fading emulator based MIMO OTA method
Agenda item:	7.1
Document for:	Discussion

1 Introduction

Recently, methodologies for MIMO over-the-air (OTA) terminal testing have been discussed in COST 2100 (SWG 2.2), in CTIA ERP (RCSG and MACSG), and in 3GPP RAN4 (MIMO OTA SI). The purpose of the MIMO OTA test set-up is to evaluate the OTA performance of multi-antenna terminals. Realistic multi-dimensional channel models are required for that purpose as discussed in [1] and in [2]. It was identified that the geometry based stochastic models (GSCM) are the most suitable for MIMO OTA testing. The GSCM include SCM, SCME, WINNER and IMT-A models [3], [4], [5]. To prepare the GSCM model around mobile terminal, a special test set-up is needed.

The high level requirements for MIMO OTA approved in Montreal [6], are defined in Section 4.3 of 3GPP TR37.976 [7]. According to the requirements, the MIMO OTA method should be able to differentiate between a good terminal and a bad terminal via over-the-air measurement of throughput. Since realistic non-isotropic radio channel is needed to differentiate between a good antenna and a bad antenna, the abovementioned GSCM models are needed and also specified in [7] as generic models. The reasoning for the GSCM models can also be found from [8], [9], [10], [11], and [12].

In 3GPP, three fundamentally different approaches have been proposed, namely reverberation chamber based methodologies, anechoic chamber based methodologies, and two-stage methods. The first two methods make it possible to evaluate the mobile terminal over-the-air end-to-end performance. However, the first method is limited to uniform angular spread of the multipath components. Therefore, only the second one fulfils the abovementioned general requirements, namely OTA test of throughput in non-isotropic channel. This paper focuses on that methodology and confirms the capability and performance of the method.

2 Methodology Description

The methodology discussed in this paper is essentially the same as one candidate in TR37.976 [7]. The MIMO OTA test setup is composed of a number of OTA chamber antennas, a multidimensional fading emulator, an anechoic chamber, communication tester / BS emulator and a device under test (DUT). The following figure depicts an example of the OTA concept. The purpose of the figure is not to restrict the implementation, but rather to clarify the general idea of the MIMO OTA concept. For simplicity, uplink cabling is not drawn here.

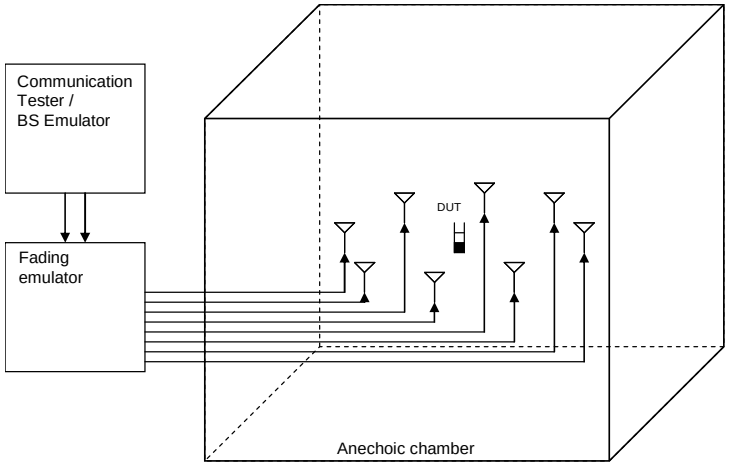

Figure 1. Example of MIMO/Multiantenna OTA test setup.

The DUT is located at center of the anechoic chamber. The idea of locating DUT into center provides a possibility to create a radio channel environment where the signal can arrive from various possible directions simultaneously to the DUT. This is the key aspect of the wideband MIMO radio channel models implemented today.

The proposed test setup is composed of a transmitter, a multidimensional radio channel emulator, an anechoic chamber equipped with OTA antennas and a DUT with multiple antennas. The crucial challenge is to generate realistic angular and polarization behavior within the anechoic chamber. The family of geometry-based stochastic channel models (GSCM) is well suitable for MIMO OTA testing. The GSCM include 3GPP SCM, SCME, WINNER and IMT-Advanced channel models. This angular and polarization behavior creates appropriate correlation at the DUT antennas. The correlation is defined implicitly via the per-path angle of arrival and real antennas. Correlation matrix based model is not suitable for this, because it includes the antenna information in the model itself.

Geometry based channel modeling methodology models BS and UE antenna arrays and the propagation between them (including angular power spectra). The parameters that are included are Doppler, Angle of Arrival, Angle of Departure, delay and polarization, which are mainly based on measurements. The measurements define certain statistics and radio channel realizations are then created by these statistical properties.

UE (DUT) antenna characteristics are assumed unknown. In other words we do not use this information in the OTA modeling.

2.1 Channel Model Mapping (Overview)

The idea of the MIMO OTA modeling is that the geometric channel models are mapped into the fading emulator. The mapping process covers all the required mathematics when converting the traditional geometric channel model to fading emulator tap coefficients as well as the calibration. The modeling process is shown in Figure 2.

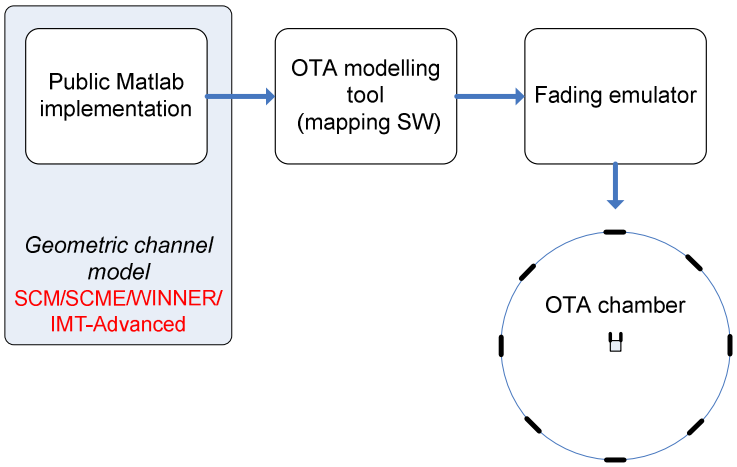

Figure 2. Channel Model Mapping.

3 Simulation and Measurement Setups

The set-up for MIMO OTA testing is depicted in Figure 3. A communication tester or a base station emulator transmits e.g. two parallel signals. A fading emulator performs convolution of Tx signals with channel model impulse responses. Fading emulator outputs are connected to a number of OTA antennas inside an anechoic chamber. OTA antennas radiate the signals to the device under test (DUT) at the centre of a ring of OTA antennas. The purpose is to generate a desired propagation environment in the test volume around DUT.

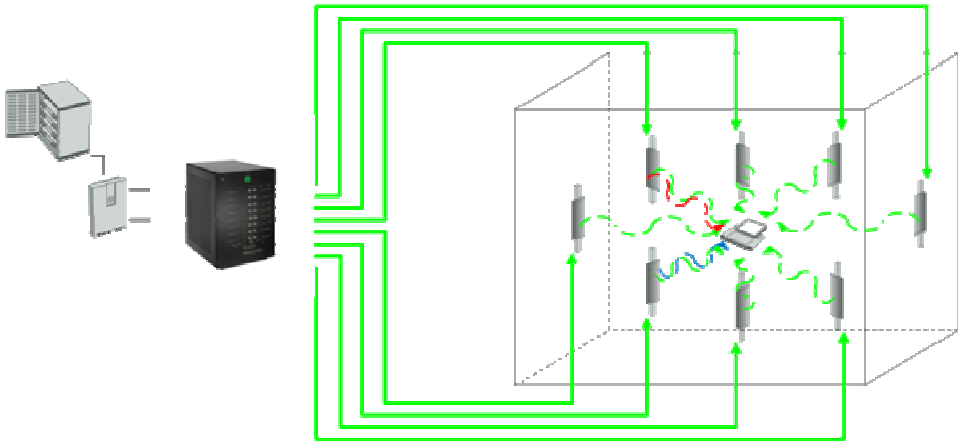

Figure 3. The MIMO OTA test set-up.

3.1 Simulation Setup

The setup for OTA simulations with Matlab™ is sketched in Figure 4. In the simulations fading signals are generated with a channel model implementation. Then the signals are weighted and mapped to OTA antennas. The signals are transmitted from a number of OTA antennas and received by a number of DUT antennas. In the following subsections characteristics of the received signals are analyzed.

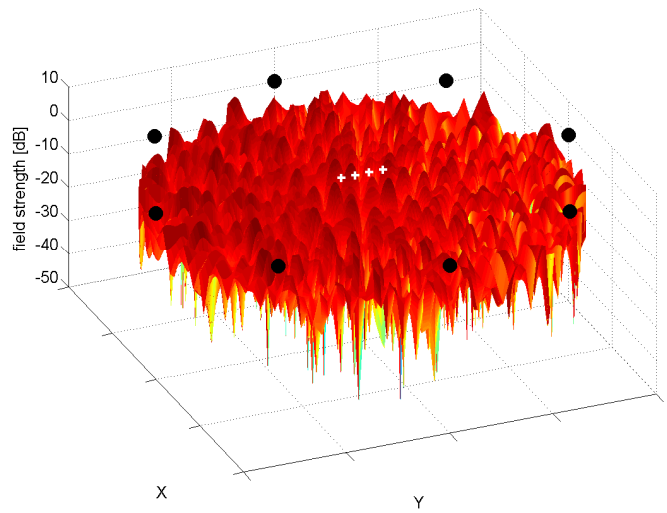

Figure 4. Illustration of the OTA Matlab simulation system.

3.2 Network Analyzer (VNA) Setup

The measurement setup included the following equipment:

Item	Quantity	Item	Details
1	**2**	**Fading Emulator**	EB Propsim F8
2	**2**	**PA**	EB OTA AMPLIFIER UNIT
3	**1**	**Signal Generator**	Hewlett Packard ESG-D4000A
4	**1**	**Spectrum Analyzer**	Agilent E4402B (9 kHz … 3.0 GHz)
5	**1**	**VNA**	R&S ZVRE (9 kHz … 4 GHz)
6	**1**	**GPIB controller**	NI GPIB-USB-B
7	**2**	**Splitter**	Mini-Circuits 15542 ZN2PD2-50
8	**2**	**GPIB cable**	1 m
9	**2**	**GPIB cable**	2 m
10	**18**	**RF cable**	H+S LIS-C9-11N-10000-41 (10 m, N to N)
11	**16**	**RF cable**	H+S Sucoflex 104E (1.5 m, N to N)
12	**4**	**RF cable**	H+S Sucoflex 104B (1 m, SMA to N)

Item	Quantity	Item	Details
13	3	BNC cable	2 m (BNC to BNC)
14	16	Dipole antenna	H+S SPA 2400/75/8/0/DS
15	2	DUT antenna	Aerial Oy AV1433-2450FN1

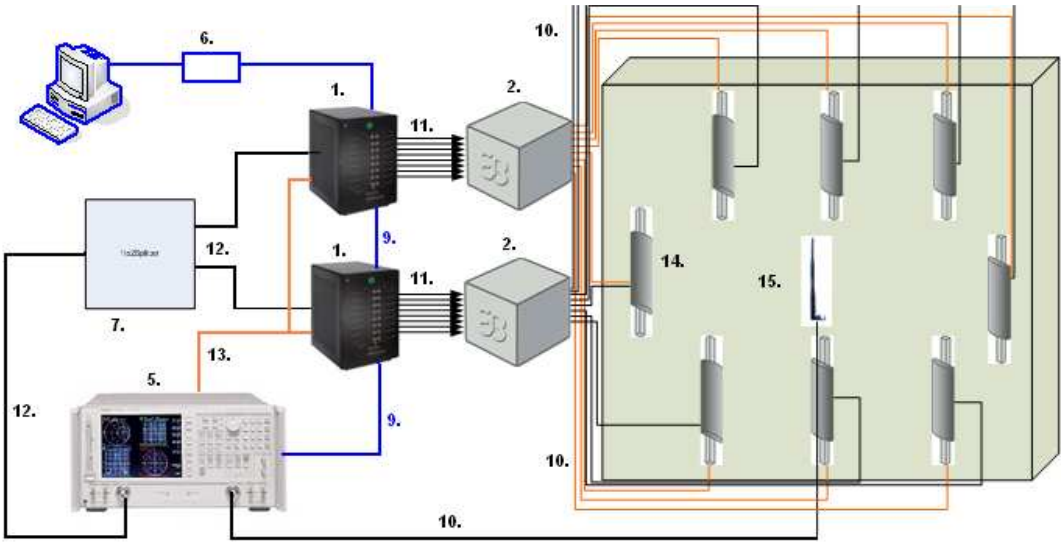

Figure 5. Measurement setup for VNA measurement.

3.3 Spectrum Analyzer (SA) Setup

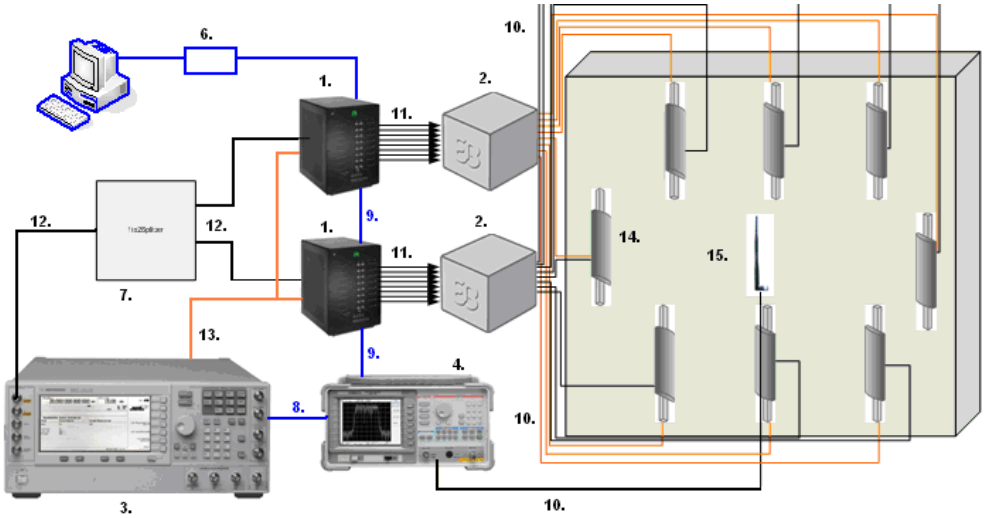

Figure 6. Measurement setup for SA measurement.

3.4 Channel Sounder (CS) Setup

OTA measurements for Power delay profiles were performed with EB Propsound™ channel sounder (Figure 7). Channel sounder operation is one-directional, from transmitter to EB Propsim channel emulators (via splitter), then to power amplifiers, probe antennas and over the air to test antenna and finally to Propsound receiver. Propsound can estimate per-path delay, Doppler, angle of departure, angle of arrival, and polarization. The estimation is done by using the SAGE algorithm.

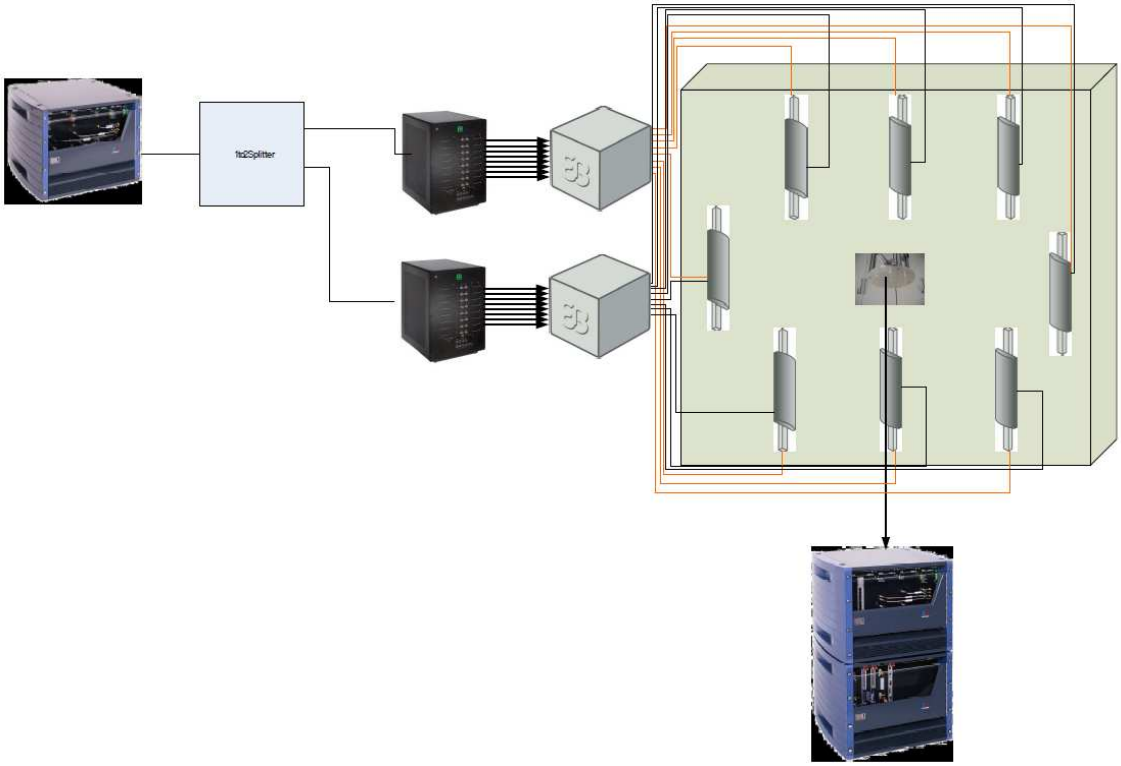

Figure 7. Measurement setup for CS measurement

4 Results

4.1 Amplitude distribution

Simulated amplitude distribution of conductive TGn model and corresponding OTA set-up is presented in Figure 8. Original TGn fading coefficients are generated by filtering complex Gaussian noise. Amplitude probability distribution functions (PDF) and cumulative distribution functions (CDF) are compared to the theoretical Rayleigh distribution which results from the isotropic scattering in the azimuth plane. The amplitude distribution follows perfectly Rayleigh distribution

as we can read from the figures. The Figure 8 shows that the MIMO OTA solution is capable to reproduce accurate Rayleigh fading.

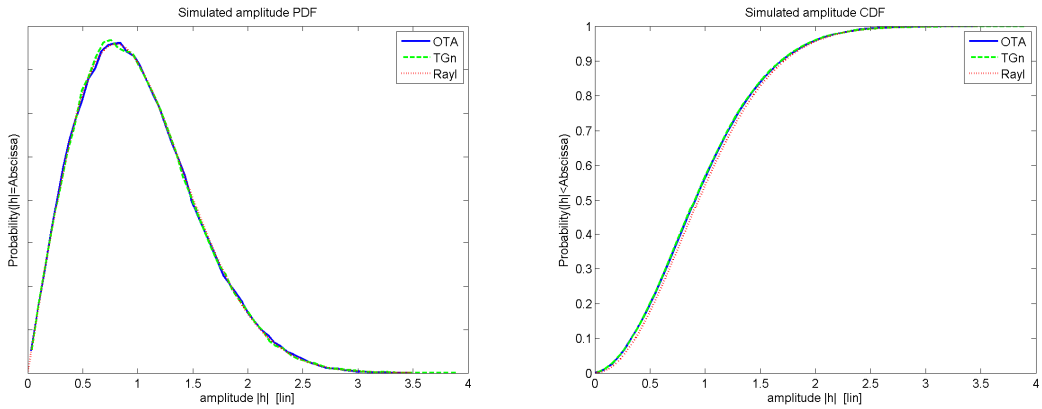

a) b)

Figure 8. Simulated and theoretical amplitude probability distribution functions (a) and cumulative distribution functions (b) of the fading coefficient.

4.2 Power delay profile

Power delay profiles (PDP) were measured by both CS and VNA setups.

PDP of SCME Urban macro and micro TDL models are illustrated in Figure 9 a) and b). The measurements were done by the channel sounder setup. The measured PDP has a good match with the original SCM TDL model PDP. Note that this measurement was done to verify the delays, not the amplitudes of the multipath components. The variation in the power of different multipaths is caused because of the non-uniform antenna pattern of the measurement antenna and different AOA of each cluster.

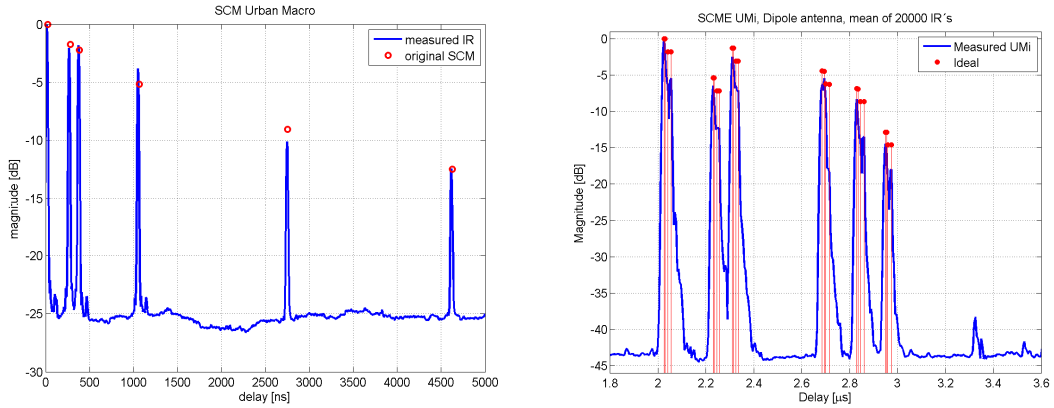

a) b)

Figure 9. Measured power delay profiles of a) SCM Urban macro and b) SCME Urban micro scenarios.

PDP was also measured by the VNA setup Figure 9. The result is shown below. In this case, the channel model had four taps in 200 ns spacing, amplitudes 0, -3, -6, and -9 dB. The measurement

result matches very well with the channel model. Again, the main focus here was to verify the delays.

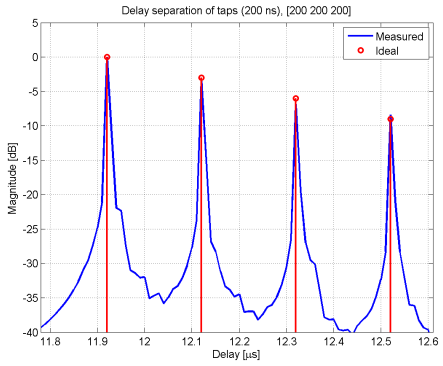

Figure 10. PDP measured by VNA.

4.3 Doppler spectrum

The measured classical Jakes and SCME Doppler spectra are shown in Figure 11 and in Figure 12, respectively. The results are as expected.

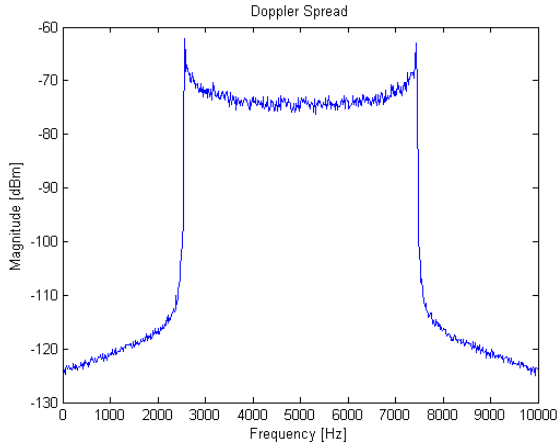

Figure 11. Classical Doppler spectrum.

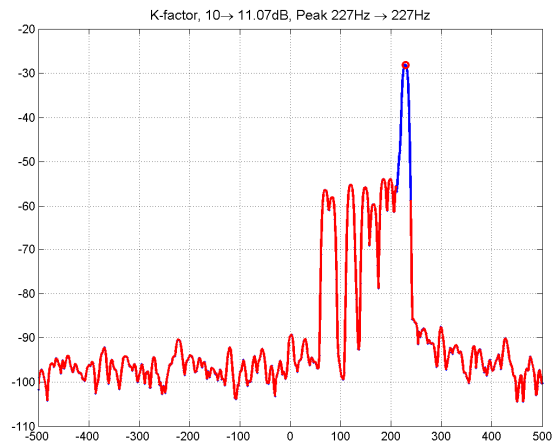

Figure 12. SCME Doppler spectrum, K = 10 dB.

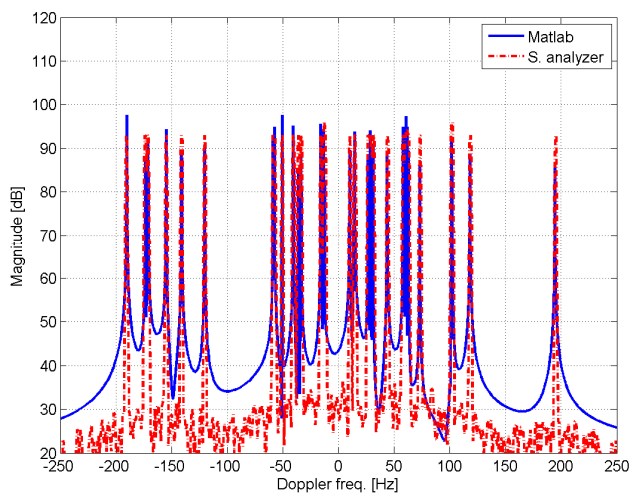

Figure 13. SCME Doppler spectrum, single cluster, NLOS.

4.4 Angle of Arrival

The worst (the most difficult) situation is when the desired angle of arrival is between the antenna probes. The desired angle of arrival is simulated by using several probes. The resulting AoA extracted from the measurement by estimating power azimuth spectrum (PAS) at DUT by applying beam steering. The received power as a function of AoA is.

$$P(\theta) = \mathbf{a}(\theta)^H \mathbf{R}_{xx} \mathbf{a}(\theta),$$

where $\boldsymbol{a}$ is the well known steering vector of antenna array and R_{xx} is the correlation matrix of received signal vector. The steering vectors are scanned over all the possible azimuth angles. The correlation matrix is recorded from the DUT itself.

PAS estimated from measurement results spectrum in various are shown in Figure 14. By visual inspection the estimated angle and the angle defined by the radio channel model is matching pretty well.

a) Desired AoA = 0°

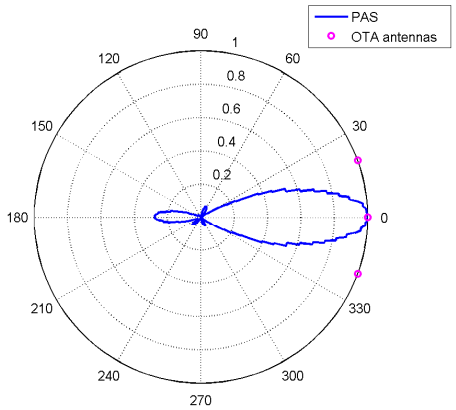

b) Desired AoA = 5°

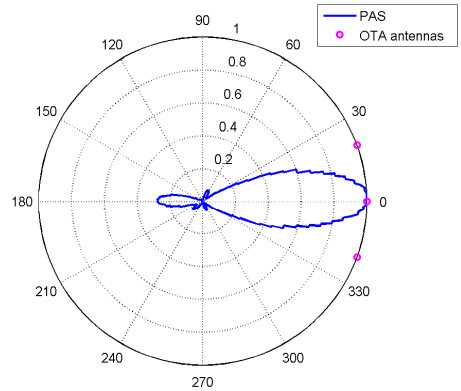

c) Desired AoA = 10°

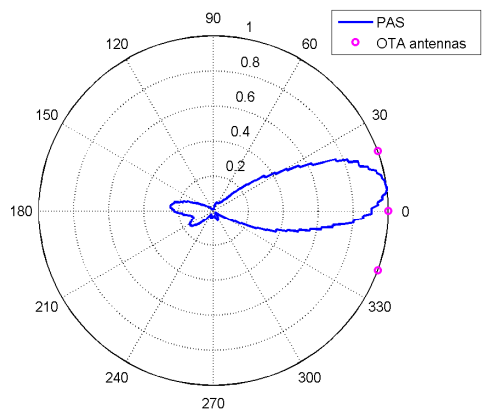

d) Desired AoA = 18°

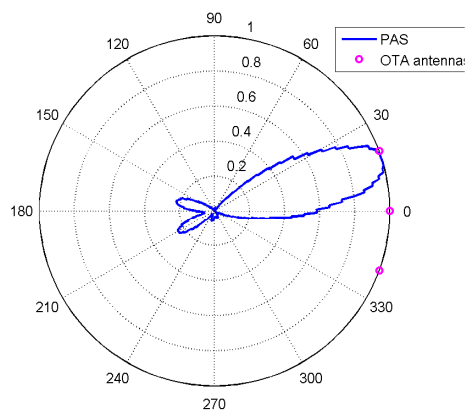

Figure 14. AoA estimates applying beam steering.

4.5 Spatial correlation

The spatial correlation function is depicted Figure 15. Four different OTA antenna configurations are simulated. Figure 15 a) has 4 OTA antennas in 90° spacing, b) 8 OTA antennas in 45° spacing, c) 16 OTA antennas in 22.5° spacing, and d) 32 OTA antennas in 11.25° spacing. In the OTA simulation an omni-directional power azimuth spectrum was modeled. OTA simulations match well with the theoretical curve.

The measured correlation for different angular spreads and different antenna spacing is shown in Figure 16. In this case a virtual array (moving antenna) was used. The measured spatial correlation proofs the concept. The measured correlation met the expectation surprisingly well since the antenna movement was handled manually. The correlation error increases when the antenna separation increases. This is aligned with the simulations shown above in Figure 15.

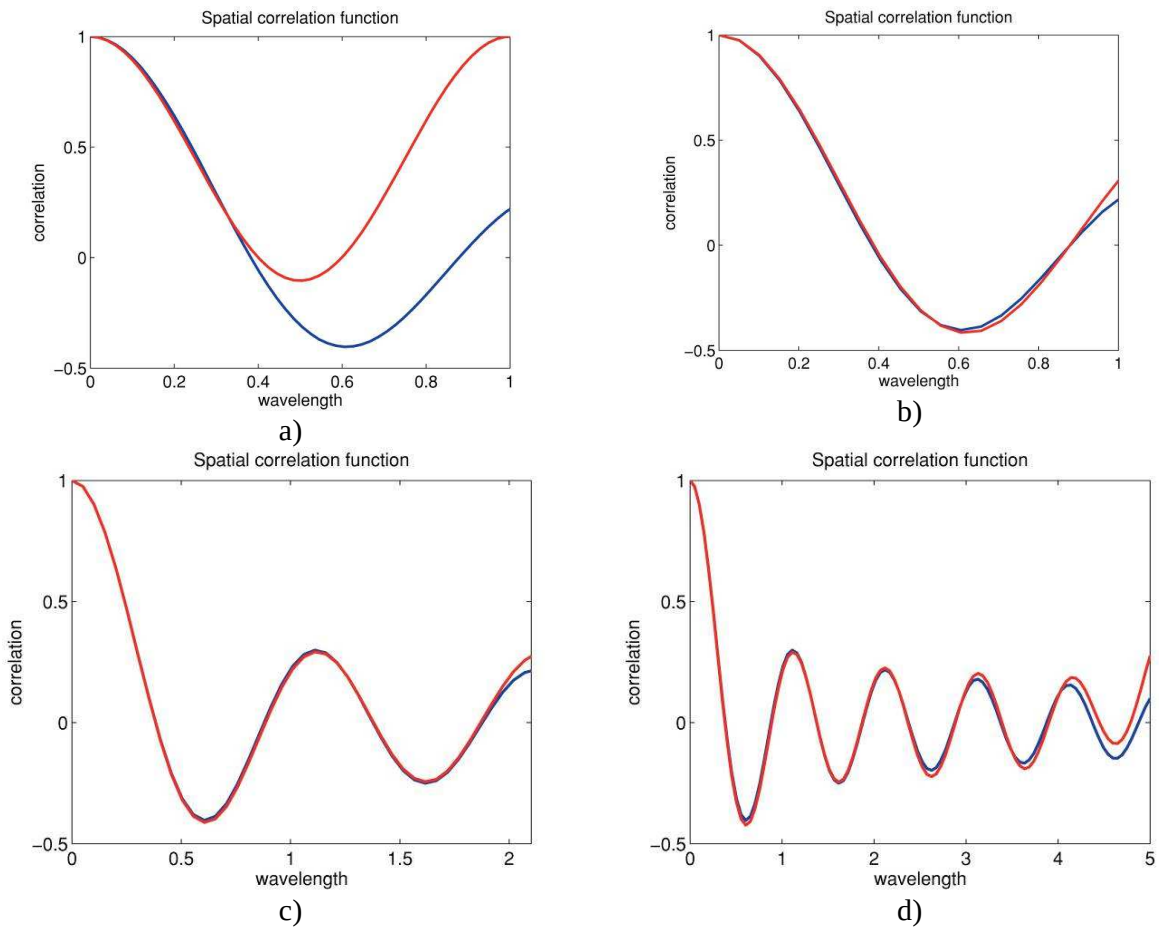

Figure 15. Simulated and theoretical spatial correlation functions.

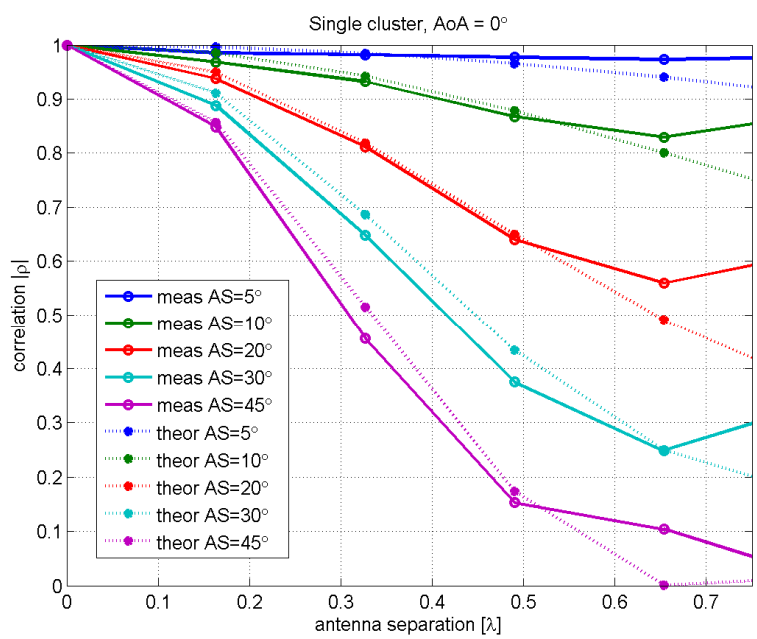

Figure 16. Measured spatial correlation.

4.6 2D Spatial correlation

To check that the correlation characteristics are similar to all directions, two-dimensional simulations were done. As long as the correlation characteristics follows the theory (is similar to all directions), the propagation environment is well in control. The size of that area is called quiet zone (i.e. free from correlation errors).

The 2D correlation for different number of OTA antennas is shown in Figure 17. We can estimate the quiet zone roughly: 0.3, 0.7, 1.8 and 4 lambdas in the cases of 4, 8, 16, and 32 OTA antennas, respectively.

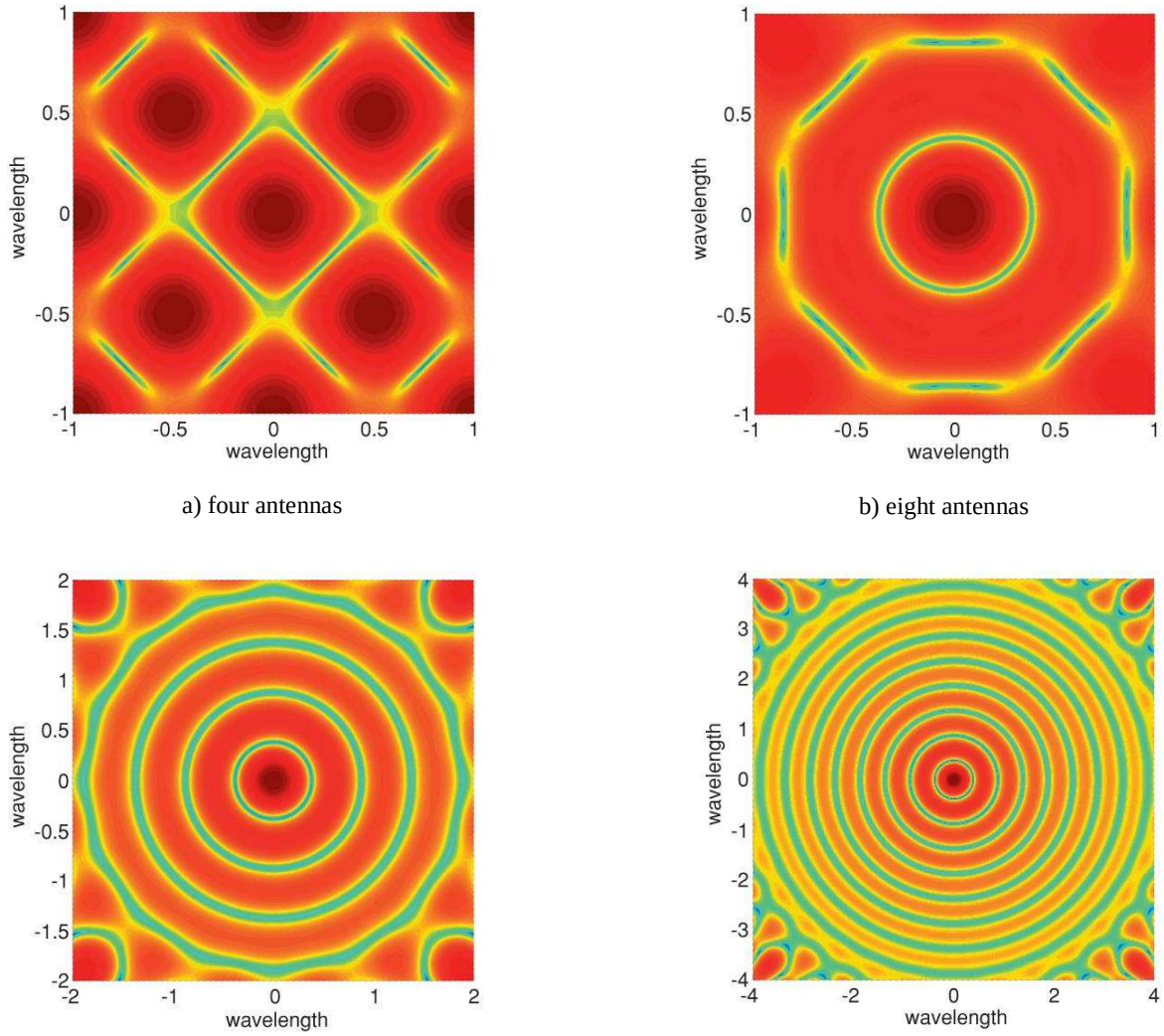

a) four antennas

b) eight antennas

c) 16 antennas

d) 32 antennas

Figure 17. 2D spatial correlation (quiet zone).

4.7 Polarization

In polarization test, we created a channel model of five cross-polarization ratio (XPR) values {20, 10, 0, -10, -20} dB. The measured XPR is shown in Figure 18.

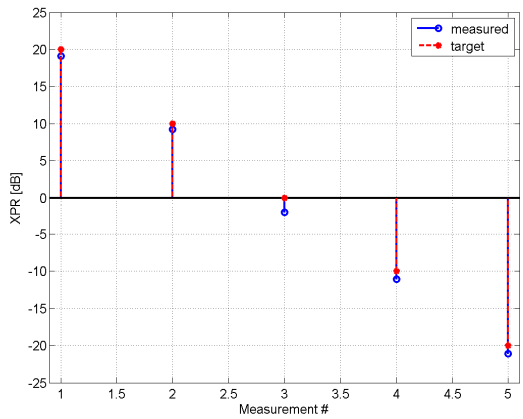

Figure 18. Measured XPR.

4.8 Throughput

Throughput was measured with WLAN access point (Figure 19, [13]), with a software defined radio platform (RACE) (Figure 20, [14]), and with two HSPA devices (Figure 21, [15]). The results show the applicability of the methodology for throughput testing. In WLAN test we can see the MIMO performance in high SNR. The performance depends on DUT rotation. In low SNRs the performance is not any more rotation selective. RACE result show that the MIMO outperforms diversity in high SNRs and diversity outperforms MIMO in low SNRs. Additionally, the RACE measurement shows that MIMO is more sensitive to antenna design than diversity. The HSPA measurement shows that device CS-15 outperforms in high SNRs and E4300 in low SNRs. The figure shows that it is possible to differentiate between devices. Which one is better, it depends on the application.

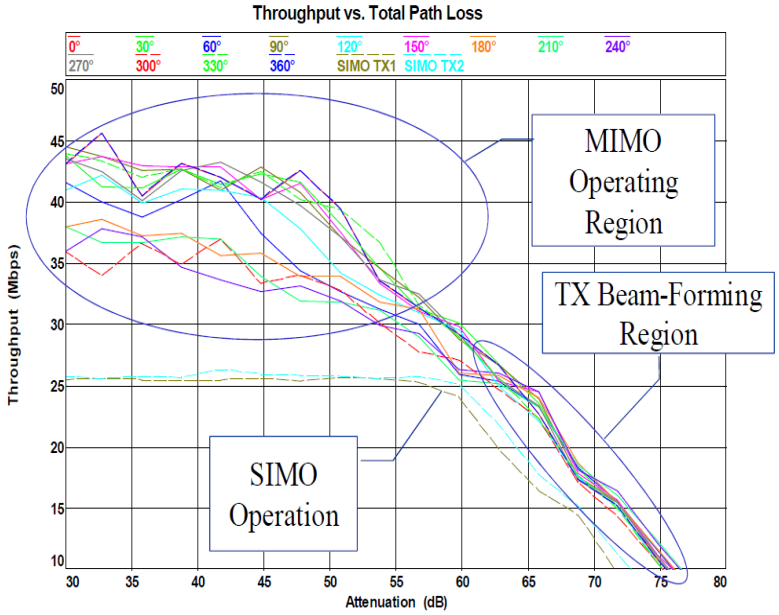

Figure 19. WLAN Test, joint work between ETS-Lindgren and Elektrobit.

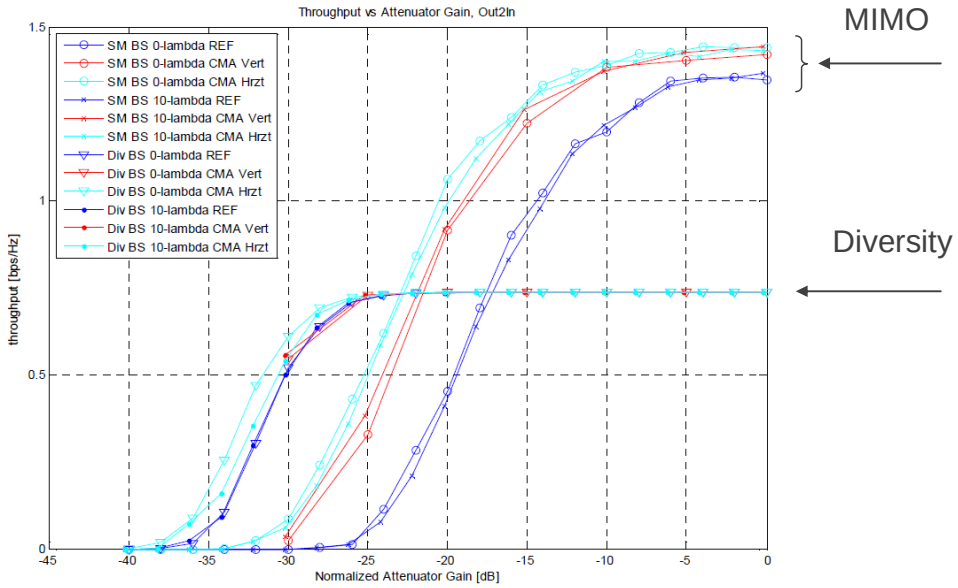

Figure 20. RACE Test, joint work between CEA-LETI and Elektrobit.

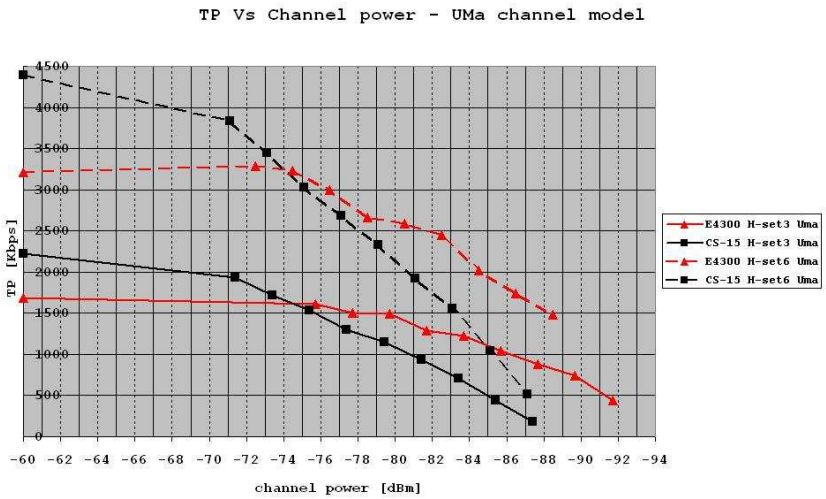

Figure 21. HSPA Throughput, measured by SATIMO.

5 Discussion and Proposal

In this paper our purpose was to demonstrate the capability of MIMO OTA set-up, depicted in Figure 3, to create the characteristics of radio channel models (SCME or TGn) inside an anechoic chamber.

The measured PDP overlaps closely to the original PDP. The simulations show that Doppler spectra match well to the corresponding spectra of reference models and conductive simulations. The measured AoA is accurate also when the AoA is between the probe antennas. Also the simulated and measured spatial correlation in the OTA case coincides well with the theoretical Bessel function. The methodology makes it possible to adjust XPR as well.

Simulations and measurements verify the capability to generate desired propagation characteristics inside the test volume using MIMO OTA set-up.

The key parameters were verified.

- Amplitude fading (Rayleigh): OK
- Doppler spread: OK
- Angle of arrival: OK
- Spatial correlation: OK
- XPR: OK
- Throughput: OK

The above verified performance confirms the fading characteristics. Basically the only uncertainty left is the power level. There is no reason to assume that the power level differs too much from SISO OTA. It can be even better since the power error is calibrated out by VNA, and the uniform EM field is ensured via the quiet zone. Therefore, we assume the whole MIMO OTA system does not provide too much additional uncertainty compared to SISO OTA.

6 References

[1] P. Kyösti, J-P Nuutinen, T. Jämsä, D. Reed, R. Borsato, “Requirements for Channel Models for OTA Multi-antenna Terminal Testing”, COST 2100 TD(09)859, Valencia, Spain, May 2009.

[2] Spirent Communications, Elektrobit, Agilent Technologies, NTT DoCoMo, “MIMO OTA Channel Models”, 3GPP contribution R4-101979, Montreal, Canada, 10-14 May 2010.

[3] 3GPP TR 25.996, "3rd Generation Partnership Project; technical specification group radio access networks; Spatial channel model for MIMO simulations (release 6)", V6.1.0.

[4] D. S. Baum, J. Hansen, G. Del Galdo, M. Milojevic, J. Salo, and P. Kyösti, “An interim channel model for beyond-3G systems: extending the 3GPP spatial channel model (SCM),” in Proceedings of the 61st IEEE Vehicular Technology Conference (VTC ’05), vol. 5, pp. 3132–3136, Stockholm, Sweden, May-June 2005.

[5] IST-WINNER II Deliverable 1.1.2 v.1.2, “WINNER II Channel Models”, IST-WINNER2, Tech. Rep., 2008 (http://projects.celtic-initiative.org/winner+/deliverables.html).

[6] Vodafone, “Revised TPs for MIMO OTA TR 37.976: Operators Requirements”, 3GPP contribution R4-101835, approved in 3GPP RAN4 meeting in Montreal, Quebec, Canada 10-14 May 2010.

[7] 3GPP TR 37.976 “Measurement of radiated performance for MIMO and multi-antenna reception for HSPA and LTE terminals” (Release 10), V1.1.0 (2010-05).

[8] Elektrobit, Spirent Communications, “Channel Models for MIMO OTA”, 3GPP contribution R4-092943, Shenzhen, China, August 24 – 28, 2009.

[9] Spirent Communications, “Evaluating Channel Models for MIMO OTA”, 3GPP contribution R4-094673, Jeju, South Korea, November 9-13, 2009.

[10] Agilent Technologies, “Proposal for WINNER II Channel Scenarios for MIMO OTA testing”, 3GPP contribution R4-094747, Jeju, Korea, 9th – 13th November 2009.

[11] Spirent Communications, Elektrobit, Agilent Technologies, “TP to TR 25-series MIMO OTA technical report (Channel Models)”, 3GPP contribution, Dublin, Ireland, 12 – 16 April, 2010.

[12] Spirent Communications, Elektrobit, Agilent Technologies, NTT DOCOMO, Vodafone, LG Electronics, “TP to TR 25-series MIMO OTA technical report (Channel Models)”, 3GPP contribution R4-101979, approved in 3GPP RAN4 meeting in Montreal, Quebec, Canada 10-14 May 2010.

[13] Elektrobit, ETS-Lindgren, “Experimental MIMO OTA throughput measurements with a MIMO device”, 3GPP contribution R4-092942, Shenzhen, China, August 24-28, 2009.

[14] L. Rudant, A. Byman, J.-P. Nuutinen, T. Jämsä, J. Meinilä, “MIMO OTA System Performance Measurement of a Compact MIMO Antenna”, COST2100 TD(10)11055, Aalborg, Denmark, 2010/June/02-04.

[15] SATIMO Industries, “MIMO OTA Round Robin Testing Campaign: SATIMO Testing Results”, 3GPP TSG RAN4 R4-103844, Xi’an, China, 11th – 15th October 2010.